On the Volatility of Oxide Defects: Activation, Deactivation, and Transformation

T. Grasser, M. Waltl* W. Goes*, Y. Wimmer*, A.-M. El-Sayed†, A.L. Shluger†, and B. Kaczer°*

*Institute for Microelectronics, TU Wien, Austria †University College London, UK °imec, Leuven, Belgium

***Abstract*— Recent studies have clearly shown that oxide defects are more complicated than typically assumed in simple two-state models, which only consider a neutral and a charged state. In particular, oxide defects can be volatile, meaning that they can be deactivated and re-activated at the same site with the same properties. In addition, these defects can transform and change their properties. The details of all these processes are presently unknown and poorly characterized. Here we employ time-dependent defect spectroscopy (TDDS) to more closely study the changes occurring at the defect sites. Our findings suggest that these changes are ubiquitous and must be an essential aspect of our understanding of oxide defects. Using density-functional-theory (DFT) calculations, we propose hydrogen-defect interactions consistent with our observations. Our results suggest that standard defect characterization methods, such as the analysis of random telegraph noise (RTN), will typically only provide a snapshot of the defect landscape which is subject to change anytime during device operation.**

I. Introduction

The first observation that oxide traps are more complicated than assumed in simple two-state models (neutral vs. charged) was made twenty-six years ago in random telegraph noise (RTN) studies [1]. There it was observed that the RTN signals could occasionally disappear and reappear, a phenomenon termed *anomalous RTN*. Although this anomaly was only observed in 4% of the defects, it was suspected that this relatively small number was primarily due to experimental restrictions and that in fact a much larger number of defects could be affected. Similar observations related to disappearing and reappearing defects have been recently made in the context of the bias temperature instability (BTI) [2, 3]. This is because charge traps responsible for RTN also form a significant contribution to BTI [4–7]. In particular, it has been shown by several groups that upon repeating charging and discharging cycles, the average number of active oxide defects in large-area devices can decrease [6–9], particularly under harsher stress conditions. However, the detailed dependencies and the nature of the chemical reactions leading to this *defect volatility* have not yet been explored. Furthermore, NBTI stress was shown to increase the noise level in large-area devices [10, 11], presumably by increasing the number of active traps producing RTN. On the other hand, in small-area devices NBTI stress can both *increase* and *decrease* the number of defects producing RTN [3].

In our recent single-defect time-dependent defect spectroscopy (TDDS) studies we have already repeatedly come across disappearing and reappearing defects [2], which were thus quite challenging to characterize [12]. So far, we had only observed defects disappearing into a neutral state. Quite recently, evidence of defects transforming into a quasi-permanent positive state was presented [13]. However, no systematic study of these intriguing phenomena is available yet. Here we summarize our efforts toward a better understanding of defect volatility and transformation, both experimentally and theoretically using TDDS and density-functional (DFT) calculations. The samples used in our study are nanoscale SiON pMOSFETs used previously [12].

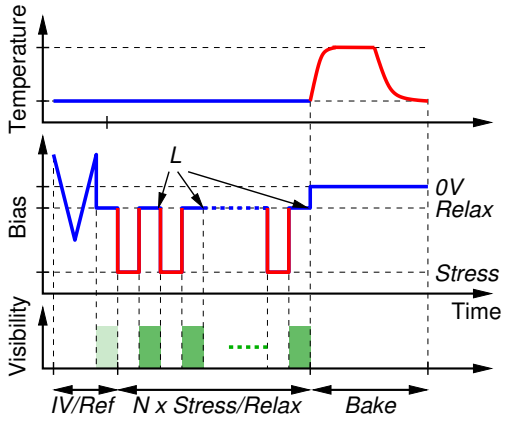

Fig. 1. **The TDDS Setup:** Initially, a reference I_D/V_G curve for the conversion of ΔI_D to ΔV_{th} and a reference trace to check for initial instabilities are measured (IV/Ref). Then, the device is stressed and recovered N times and the recovery traces are analyzed for discrete steps. The last value of the recovery trace, L, provides an indication about 'permanent' changes in ΔV_{th}. Optionally, a bake step is introduced, typically at 350°C to presumably anneal the device.

II. Experimental

In our previous TDDS studies, defects have been mainly analyzed in terms of the bias and temperature dependencies of their capture and emission times (τ_c and τ_e). These time constants are widely distributed and definitely extend well outside feasible experimental windows of microseconds up to hours [2, 11, 14]. Volatility and transformations typically occur on much larger time scales and have so far been considered parasitic second-order effects. As of yet, however, no dedicated experiments have been performed to further elucidate these processes.

In typical TDDS experiments the stress/recovery voltages and times as well as the temperature are varied over wide ranges dictated by the primary goal of extracting the bias and temperature dependence of the time constants. However, in order to best study defect transformation processes it appears more sensible to repeat the same experiment at constant stress/recovery voltages, times, and temperatures over and over again for many days to allow for the detection of changes in the defect behavior. In our case, we used moderate stress voltages (typically $-1.7\,\mathrm{V}$, corresponding to an oxide field of

978-1-4673-7362-3/15/$31.00 ©2015 IEEE

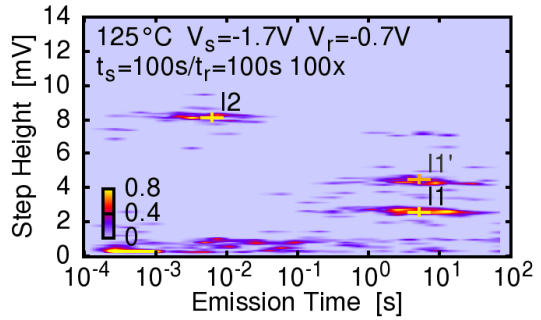

Fig. 2. Example TDDS spectral map for device I. Defect I1 was stable for the duration of the measurement (4.5 days, repeated 1 to 100s stress, 1 to 100s recovery, $\approx 5\,\mathrm{MV/cm}$), defect I2 was strongly volatile.

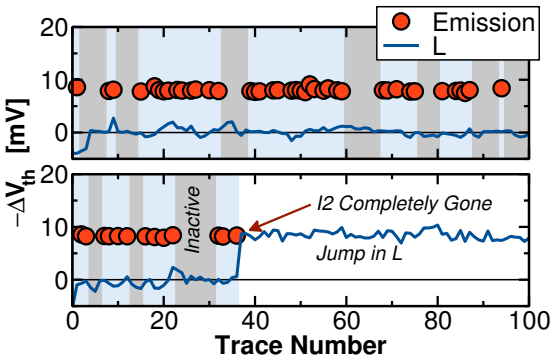

Fig. 3. **Top**: Typical emission pattern of defect I2 during the first 1.5 days ($t_s/t_r = 100\,\mathrm{s}/100\,\mathrm{s}$ with $\tau_c = 400\,\mathrm{ms}$). A red circle means that the defect emitted a charge after a stress pulse. Since the stress time was 250 times longer than the average capture time, the capture probability would be close to 1. The gray areas highlight the traces where no emission was recorded from this defect despite the large capture probability. The blue line shows L, the value of ΔV_{th} at the end of the recovery trace (at 100 s in the above case) **Bottom**: After 1.5 days, I2 disappeared and a permanent contribution in L of the same magnitude was observed, meaning that I2 likely transformed into a fixed positive charge.

about $5\,\mathrm{MV/cm}$) and temperatures (125°C) in order to provide information relevant at use conditions. This TDDS setup is schematically shown in Fig. 1 together with an optional bake step, all automatically performed in a computer-controlled mini-furnace. The optional bake steps, typically performed for 1h at 350°C, are motivated by the observation that in large-area devices such a bake restores the initial state prior to degradation [15, 16]. Furthermore, it has been observed that upon repeated stress/recovery cycling the amount of recoverable defects typically decreases with time [6, 7, 9, 17, 18], which is the macroscopic (large area) equivalent of defect volatility. In large-area devices it has been found that baking can also reverse this net loss of defects [12]. As those baking studies have been performed on large-area devices, we may expect this to also hold in small-area devices, at least on average.

III. Results

The defects visible in a few devices were monitored on average for several weeks each, using a TDDS scheme as shown in Fig. 1. An example TDDS spectral map of device 'I' with two dominant defects is shown in Fig. 2. Even in a

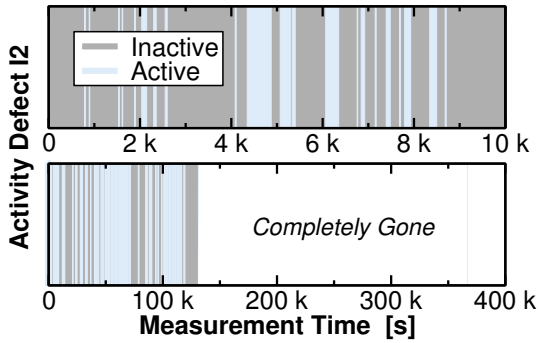

Fig. 4. The emission pattern of defect I2 shown in Fig. 3 but on larger time scales. **Top**: Initial experiments with shorter stress/relaxation times ($t_s/t_r = 1\,\mathrm{s}/10\,\mathrm{s}$). **Bottom**: The activity of I2 during the whole experiment on device I: after an initial phase of strong volatility, I2 transformed into a fixed positive state.

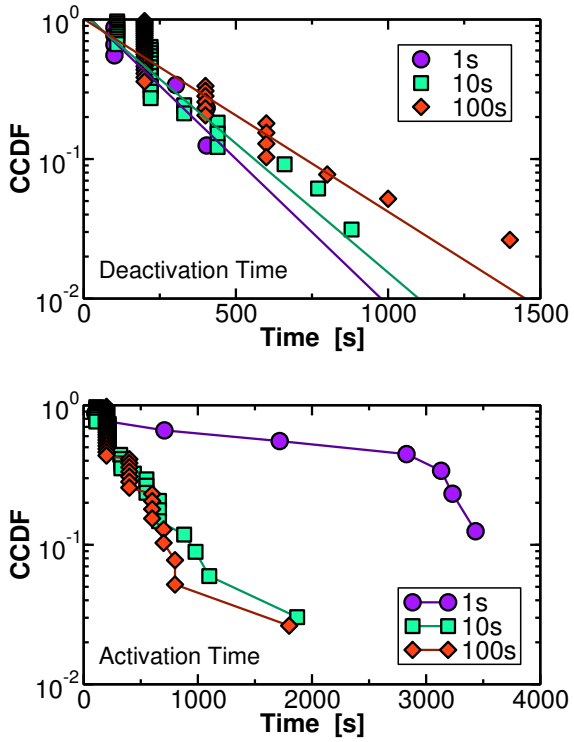

Fig. 5. The complementary cumulative distributions (CCDFs) of the extracted deactivation/activation times of defect I2 appear to depend on a combination of stress and recovery times. In the above experiments, the recovery times were always 100 s while the stress times were varied between 1 and 100 s. While the deactivation times are roughly independent of t_s and follow an exponential distribution ($\tau \approx 210$, 230, and 310 s), activation appears to require at least a stress of about 10 s.

relatively short time span of a couple of weeks per device only 40% of the defects showed no volatility. The defects that did show volatility did so on widely distributed timescales, starting from defects that were deactivated and reactivated within hundreds of seconds up to those which simply disappeared or appeared after weeks (or many months, as seen previously [12]).

As an example of a highly volatile defect, defect I2 (capture/emission times of 10 ms/1 s) is shown in Fig. 3. I2 had

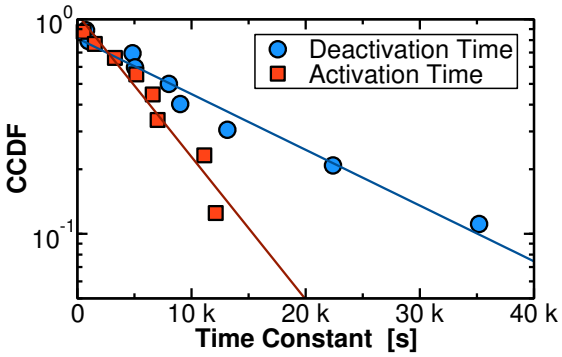

Fig. 6. Volatility was found to occur on widely distributed timescales. For example, the volatility of defect K2, which was significantly less frequent than that of I2, can also be well fitted by an exponential distribution, consistent with a *reaction-limited* process [19, 20].

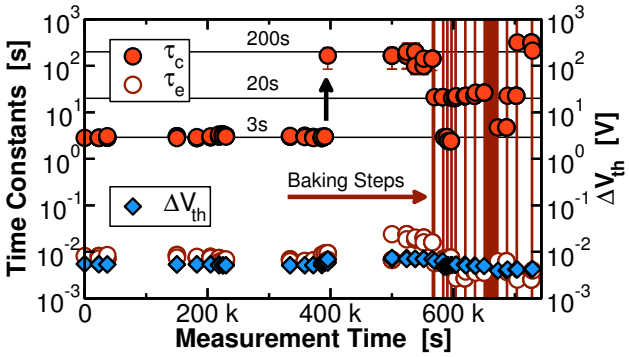

Fig. 8. Transformations of J1 during 8 days of measurement. After 4.5 days, τ_c changed spontaneously from 3 s to 200 s (see Fig. 7) and remained stable for 2 days. By repeatedly baking for 1h@350°C, τ_c could be randomly switched between 3 s, 20 s, and 200 s.

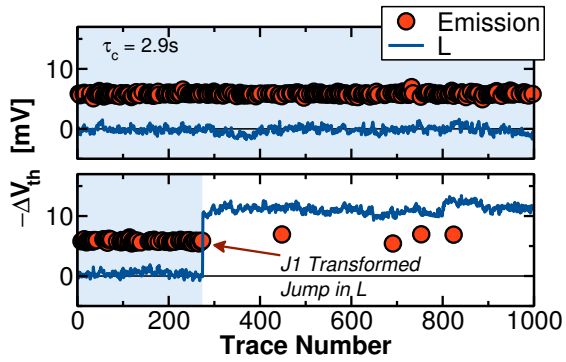

Fig. 7. **Top**: Typical emission pattern of defect J1 during the first 4.5 days. **Bottom**: After about 4.5 days, defect J1 disappeared and a nearly twice as high permanent contribution to L was created, possibly a depassivated Si-H bond at the interface (P_b-center) [21, 22].

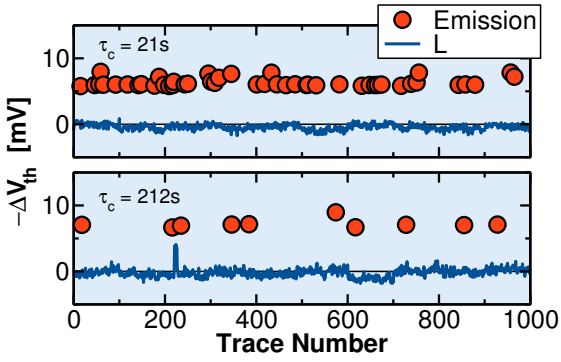

Fig. 9. Two other typical emission patterns of defect J1 observed in between bake steps. **Top**: The state with $\tau_c \simeq 20$ s, which was most often observed (55%). **Bottom**: The state with $\tau_c \simeq 200$ s was least frequently observed (18%). Compare this to the initial state with 3 s (27%) as shown in Fig. 7.

widely distributed activation and deactivation times averaging around 1 ks. In particular, I2 was activated/deactivated more than hundred times before it 'permanently' disappeared into a positive state, see Fig. 4. Interestingly, this positive state had the same contribution to ΔV_{th} as the active defect, indicating that both the active defect as well as the permanent positive charge are at the same location. The recorded distributions of this fast activation/deactivation process are shown in Fig. 5. Interestingly, the deactivation time of this defect was exponentially distributed with the mean depending only weakly on the stress time. This would be consistent with a defect reaction occurring at the defect site that is not limited by the availability of other reactants. The (re)activation time, on the other hand, was found to be exponentially distributed only for stresses longer than about 10 s. As an example for a defect with much larger activation/deactivation times, defect K2 is shown in Fig. 6. We note that as these changes are most likely thermally activated processes [12], these times specific to 125°C will be much longer at room temperature.

As an example for an apparently regular defect which initially showed no signs of volatility, defect J1 is shown in Fig. 7. After 4.5 days, however, it suddenly seemed to have disappeared, triggering a significantly higher ΔV_{th} in the last value of each trace, L. At closer inspection (by increasing the number of traces from $N = 100$ to $N = 1000$), the occasional emission events of the same step-height as those of J1 could be identified as a regular first-order process with an about 66% larger capture time but roughly the same emission time as that of the original J1. We assign these events, which were stable for 2 days, to a transformed J1. When checking whether baking could restore the initial J1, we found another value of τ_c, now at 20 s. Interestingly, the 11 subsequent bake steps randomly cycled τ_c between the values 3, 20, and 200 s, see Figs. 8 and 9. Similar behavior was seen quite regularly in other devices. This included defects which could be cycled between 2-3 'configurations', defects which could not be charged once for a long time, and cases where the defects appeared sometime during the experiment (and possibly also disappeared at a later point).

Yet another behavior was seen in defect J2: this defect, when left at the recovery voltage for a long enough time (about 10 s), spontaneously transformed into a fixed positive state, see Fig. 10. While this transformation could be prevented by a quick re-stress, once transformed, the defect no longer reacted to the TDDS charging/discharging voltages, see Fig. 11. We observed that the time needed for transformation could be significantly reduced at more negative gate bias, cf. Fig. 12. Intriguingly, the transformed positive defect could be reactivated by a short pulse into accumulation (e.g. 1 V for 1 s), likely due to an electron capture event, see Fig. 13. After 18 such re-activations, J2 disappeared into a *neutral* state and could not be restored even by 32 bake steps.

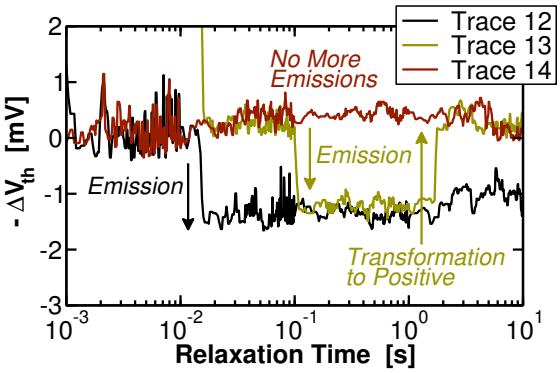

Fig. 10. Defect J2 showed a rare kind of volatility: from the neutral activate state, the defect could transform into a fixed positive state in about 1-5 s. This could be prevented by keeping the relaxation time short.

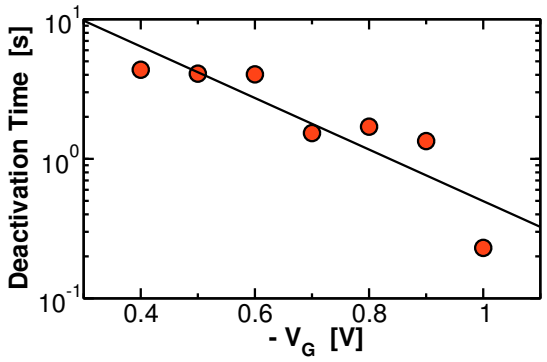

Fig. 12. The average transition time into the fixed positive state of J2 decreases exponentially with increasing negative bias. This is consistent with the idea that this process is related to hole trapping from the channel.

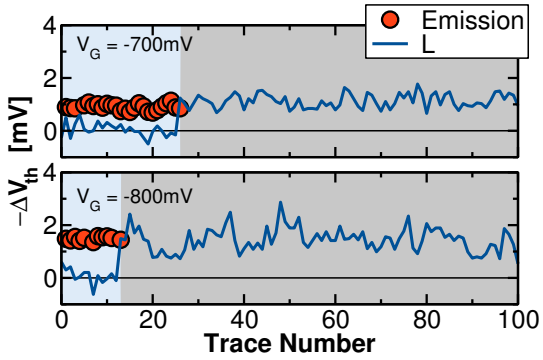

Fig. 11. Two TDDS measurements of J2 taken at different readout voltages. Once a transition into a fixed positive state occurred (visible in the last value of the recovery trace, *L*), J2 no longer reacted to charging/discharging cycles.

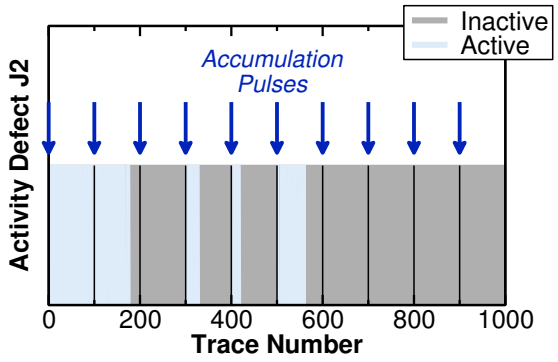

Fig. 13. Using a pulse into accumulation, we could 18 times reactivate J2 from the fixed positive state into the active state (10 examples pulses shown above, 5 of them successfully reactivating the defect). Then, J2 disappeared into a neutral configuration and could not be reactivated even by 32 bake steps.

IV. Discussion

We summarize the rich spectrum of experimentally observed features:

(i) Most defects showed volatility, ranging from relatively fast changes (kiloseconds on average) up to many weeks (and probably longer if we had taken more time to wait).

(ii) Even though the activation/deactivation times were found to be relatively large and therefore the number of recorded events small, the process seems to be consistent with a *reaction-limited* process.

(iii) Defects can become temporarily inactive both in a neutral and a positive state. From that temporarily inactive state, some defects may be activated for instance by a bias pulse toward accumulation (electron injection).

(iv) The capture time constants of defects can change, either spontaneously or as a response to a bake step. While it is conceivable that *both* the capture *and* the emission time of a defect change, identification of such a scenario is more difficult, since the emission time is a primary fingerprint in spectral maps such as the one shown in Fig. 2.

(v) And finally, defects can permanently disappear, also both into a neutral and a positive state. Once disappeared, it may be possible that the defect is reactivated either by a bake step or by chance/spontaneously. However, in some cases even a larger number of bake steps did not reactivate the defect. Whether this a consequence of insuffient baking (too short or with a too low temperature), or another fundamental effect remains to be clarified.

All of the above listed changes at the defect site strongly suggests an involvement of the ubiquitous hydrogen, which has been linked to various reliability issues [24–29]. Also, in our previous DFT studies [12, 23] where we compared theoretical predictions to TDDS experiments, we have identified hydrogen-related E'-centers as interesting defect candidates. One of these candidates, the hydroxyl E'-center [30], is shown in Fig. 14 (right) together with a few possible ways it may interact with H and H_2 (left). In particular, arrival of H^0 will passivate the defect while the arrival of another H^0 will reactivate it and release H_2.

The primary question here relates to the source of atomic or molecular hydrogen. It has been shown a long time ago that atomic hydrogen either dimerizes or binds to some oxide sites at temperatures larger than about 130K [31] and should therefore not exist as a free agent in our experiments. Nonetheless, it has been confirmed many times that even 'dry' oxides contain a massive amount of hydrogen, possibly in the excess of 10^{18} or even $10^{19}\,\mathrm{cm}^{-3}$ [31, 32], albeit in bound form. A number of experiments have suggested that some of this hydrogen *can* be released as H^0 during bias temperature

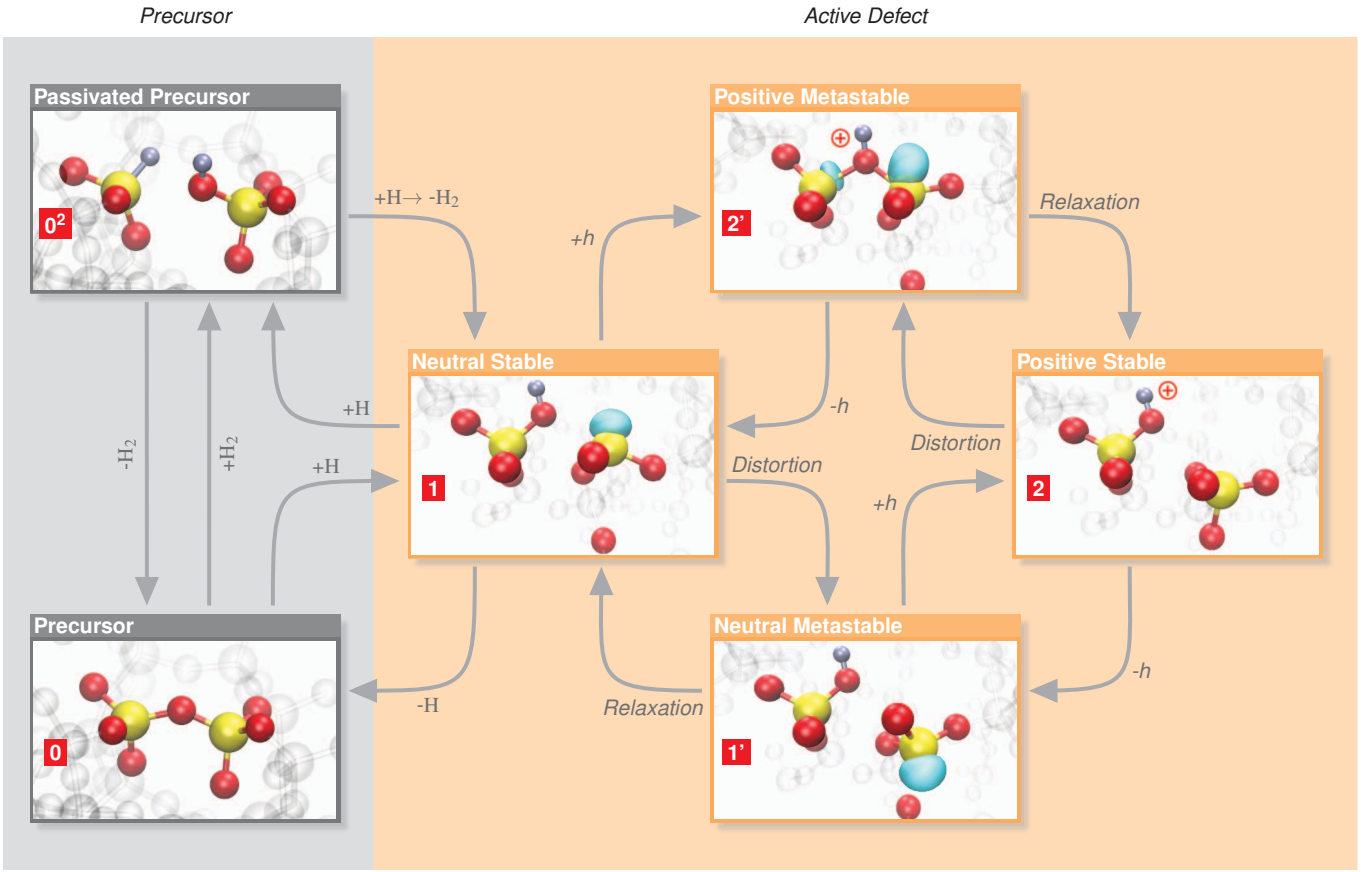

Fig. 14. Two possible precursor states of the hydroxyl E' center: the precursor may be either decorated with two hydrogen atoms (top) or none (bottom). Shown are also possible mechanisms that activate the defect by interaction with atomic or molecular hydrogen.

The four states of the hydroxyl E' center: In the neutral configuration 1, a hydroxyl group sits at the left Si while the other carries a dangling bond. After hole capture, in state 2', the dangling bond has lost its electron and reforms the Si-O-Si bridge, resulting in the typical proton sitting on a bridging O. In state 2, the right Si moves through the plane of its O neighbors, forming a bond with the O in its back. In state 1', the dangling bond is restored but points into the other direction. By various interactions with hydrogen the defect can be transformed into a precursor state (left). Only the most likely interactions according to DFT are shown, e.g. the transition from 0^2 to 1 by the release of H is omitted (see the large barriers in Fig. 15).

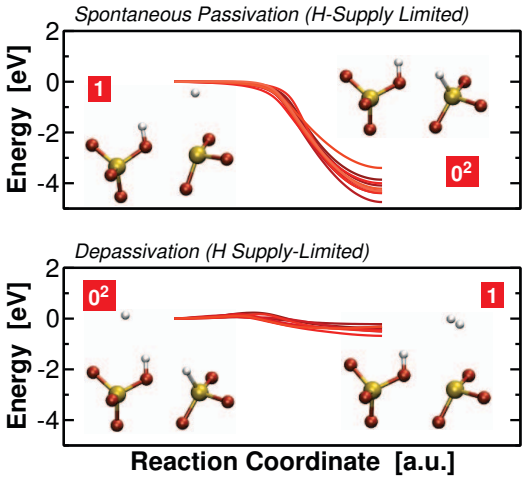

Fig. 15. Interactions of H with a hydroxyl E'-center[23], as per DFT calculations in an amorphous oxide for various defect sites. **Top**: H can spontaneously passivate active defects (transition $1 \rightarrow 0^2$). **Bottom**: Another H can (with a negligible barrier) re-activate the defect again (transition $0^2 \rightarrow 1$).

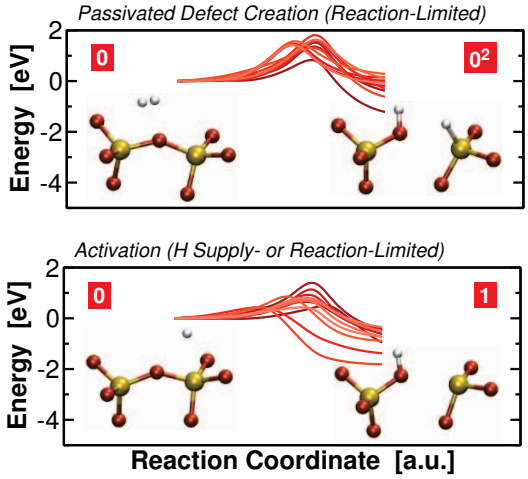

Fig. 16. **Top**: At strained Si-O bonds (bonding distance > 1.65Å), H_2 can create a passivated defect. Arrival of H would activate that defect (transition $0 \rightarrow 0^2$), see also Fig. 15. **Bottom**: H can also react with these strained Si-O bonds to create an active defect, a hydroxyl E'-center (transition $0 \rightarrow 1$).

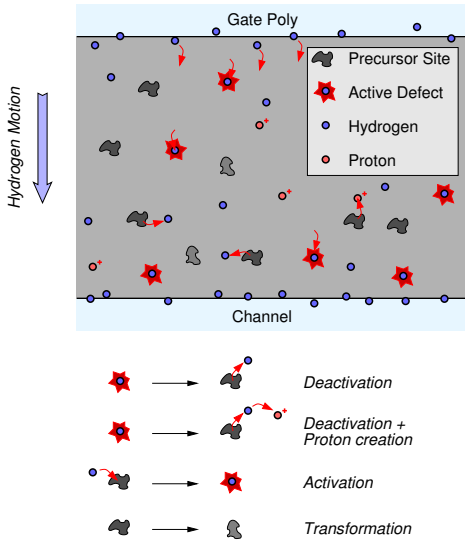

Fig. 17. Simplified schematics of some relevant processes. Not shown is the fact that *all* defect sites are different. Nuclear reaction analysis demonstrates [38, 41] that H moves from the *gate* towards the channel during NBTI stress. Not shown are the interface states created at the channel interface during long-term stress.

stress, most likely from the *gate interface* of the oxide, see the classic 'hydrogen-release' models [21, 33–35]. This hydrogen can then move towards the channel [36–38] where it can interact with defects and channel-dopants in numerous ways.

In order to check the plausibility of this hypothesis, we performed DFT calculations in large amorphous SiO_2 structures containing 216 atoms. The structures were created using ReaxFF [39] and optimized using a non-local PBE0_TC_LRC hybrid functional as implemented in the CP2K code [40]. According to these DFT calculations, see Fig. 15, atomic hydrogen can spontaneously passivate the dangling Si bond at the hydroxyl E'-center [23]. Although this process could in principle be diffusion-limited if the barriers for the hydrogen-defect reactions are small, reported diffusion constants of H and H_2 are so large [31] that it is unlikely that such cases can be resolved experimentally. We therefore speculate that the measured activation/deactivation times are either limited by the time taken to release hydrogen for instance at the gate interface or by the barrier at the defect site preventing the reaction. Once the defect is deactivated by a hydrogen reaction, another H reaching the site would re-activate that defect again [30], see defect I2. Alternatively, H_2 and H could attack a strained Si–O bond to form an active defect/passivated precursor (Fig. 16) which could create a new defect at a suitable precursor site. Although the barriers vary significantly from site to site, they are relatively large with about 1-2 eV, making such a process rather reaction- than diffusion-limited.

This finally lets us arrive at the picture shown in Fig. 17: defects are either present or can be created at suitable precursor sites, such as strained Si–O sites, by the incorporation of H. Subsequent reactions with mobile H/H_2 can either passivate defects, activate previously passivated defects, or create defects in initially unoccupied sites. The released H could capture a hole and get trapped nearby the defect site, as for instance in defects J1 and J2. Finally, given the flexibility of the SiO_2 network, local rearrangements at defect sites are possible, which primarily affect the time constants.

V. Defect Creation vs. Activation

One observation that has repeatedly created confusion and controversy in BTI literature is the creation of new defects during stress [3, 29]. Our experiments shed new light on the matter: starting from the pristine sample, the defects observable in TDDS, namely those contributing to BTI recovery, have been well characterized in terms of the bias/temperature dependence of their capture/emission times. While the experiment progresses, some defects disappear (become deactivated) and some new ones are created. Whether these new defects are really new in the sense that they are created in some region damaged by the stress or whether they are simply activated at some precursor site like other defects showing volatility is hard to say with any certainty. However, to the best of our knowledge, their properties are identical to those existing in the pristine sample, that is, they have similar capture and emission times. As such, they can also contribute to stress-induced leakage currents in a similar manner [42], thereby possibly contributing to progressive oxide breakdown. As such it appears to be *better to speak of defect activation at pre-existing precursor sites rather than the creation of completely new defects anywhere in the oxide*.

Suitable precursor sites would be strained Si-O bonds, which are the precursors of the defect shown in Fig. 14. A large number of precursor sites and defect candidates are in principle conceivable and have also been studied in literature. However, from all the defect candidates we have investigated so far [23], the hydroxyl E' center appears to be most consistent with experiment.

We finally note that since our experiments indicate that these newly created defects can show the same volatility as those already existing in the unstressed example, it appears that the time-zero-defects are a more-or-less random selection of defects possible in a particular oxide matrix. It also seems that by repeated baking it is possible to "reshuffle" the active defects between a limited number of possible candidates/configurations.

VI. Comparison to Previous Experiments

In the dedicated experiments performed here we noticed that volatility was observed in the majority of defects. This is somewhat in contradiction to our previous results obtained using a different experimental setup where volatility was rather the exception than the norm [2, 43]. After a thorough comparison of the two setups it was found that the increased volatility observed in the new experiments is a consequence of overly generous $I_D V_G$ sweeps which also extended into accumulation (+1 V), which was not the case in our previous setup. During these sweeps, electrons are created in the channel and are able to neutralize the defects. After limiting the sweep range from +0.2 to −1 V and repetition of the experiment on a new sample, all six defects visible there remained stable for about 10 days without any sign of volatility. The fact that

volatility is observed following a sweep into accumulation is reminiscent to literature results showing that carrier injection after BTI stress can lead to a considerable increase in the number of created interface states [21, 33–35, 44]. Irrespective of the practical relevance of such biasing schemes, the fact that most defects *can in principle be volatile* provides a strong clue towards the chemical nature of the most important defects. In particular, this mechanism appears consistent with a hydrogen release process at the *gate/oxide interface* [21, 33–35].

VII. Not a Reaction-Diffusion Mechanism

At a first glance, the hydrogen-induced defect volatility may trigger associations with the reaction-diffusion model [29, 45], in which hydrogen is assumed to be released from the *channel* interface to quickly diffuse through the oxide and then onwards through the gate poly. The mechanism invoked here, however, is *entirely different*. First of all, the measured degradation remains to be due to a collection of first-order processes rather than a diffusion process, consistent with our previous experimental results on small-area devices [2, 20]. The interactions with hydrogen invoked to explain the volatility are merely *parasitic* effects. Second, hydrogen is assumed to be released at the *gate* interface rather than the channel interface and assumed to diffuse very quickly towards the channel, consistent with classic hydrogen-release models for time-dependent dielectric breakdown [46]. In these models the time needed for hydrogen diffusion is not rate-limiting, consistent with the high diffusivity of H and H_2 in SiO_2[31]. Also note that the hydrogen motion would be in the opposite direction of what is assumed in the reaction-diffusion model. However, hydrogen motion towards the *channel* interface is consistent with the observed passivation of dopants in the channel [36] and the observed motion of hydrogen in nuclear reaction analysis [38, 41]. Furthermore, this direction would be consistent with the observed creation of interface states [21, 22] via a reaction of the form $\mathrm{Si-H+H \rightarrow Si-^{\bullet}+H_2}$, which cannot be otherwise explained by pure interaction with inversion layer holes as the barriers would be too large [47, 48]. In any case, the assumed interactions with hydrogen leading to parasitic effects such as volatility are admittedly speculative at present and will require further investigation.

VIII. Conclusions

We have shown that most defects responsible for the recoverable component of BTI can show volatility. The number of defects showing volatility appears to increase significantly when the device is occasionally driven towards accumulation. The wide range of observed changes at the defect sites could be explained by invoking interactions of hydrogen with precursors in the SiO_2 network, whereby the hydrogen is preferentially released by those accumulation sweeps. While the impact of volatility may average out in large devices, characterization of the initial defect configurations in nanoscale devices such as SRAM cells can only provide a snapshot of the current state and the impact of volatility and transformations must be considered.

Acknowledgments

The research leading to these results has received funding from the Austrian Science Fund (FWF) project n°26382-N30 and the European Community's FP7 project n°619234 (MoRV) as well as the Intel Sponsored Research Project n°2013111914. The computational results presented have been achieved in part using the Vienna Scientific Cluster (VSC) and the UK's national high-performance computing service HECToR and Archer via the Materials Chemistry Consortium (EPSRC EP/F067496).

References

[1] M. Uren, M. Kirton, and S. Collins, "Anomalous Telegraph Noise in Small-Area Silicon Metal-Oxide-Semiconductor Field-Effect Transistors," *Physical Review B*, vol. 37, no. 14, pp. 8346–8350, 1988.

[2] T. Grasser, H. Reisinger, P.-J. Wagner, W. Goes, F. Schanovsky, and B. Kaczer, "The Time Dependent Defect Spectroscopy (TDDS) for the Characterization of the Bias Temperature Instability," in *Proc. Intl.Rel.Phys.Symp. (IRPS)*, May 2010, pp. 16–25.

[3] T. Grasser, K. Rott, H. Reisinger, M. Waltl, J. Franco, and B. Kaczer, "A Unified Perspective of RTN and BTI," in *Proc. Intl.Rel.Phys.Symp. (IRPS)*, June 2014, pp. 4A.5.1–4A.5.7.

[4] J. Zhang, C. Zhao, A. Chen, G. Groeseneken, and R. Degraeve, "Hole Traps in Silicon Dioxides - Part I: Properties," *IEEE Trans.Electron Devices*, vol. 51, no. 8, pp. 1267–1273, 2004.

[5] V. Huard, M. Denais, and C. Parthasarathy, "NBTI Degradation: From Physical Mechanisms to Modelling," *Microelectronics Reliability*, vol. 46, no. 1, pp. 1–23, 2006.

[6] T. Grasser, P.-J. Wagner, H. Reisinger, T. Aichinger, G. Pobegen, M. Nelhiebel, and B. Kaczer, "Analytic Modeling of the Bias Temperature Instability Using Capture/Emission Time Maps," in *Proc. Intl.Electron Devices Meeting (IEDM)*, Dec. 2011, pp. 27.4.1–27.4.4.

[7] M. Duan, J. Zhang, Z. Ji, W. Zhang, B. Kaczer, S. De Gendt, and G. Groeseneken, "Defect Loss: A New Concept for Reliability of MOSFETs," *IEEE Electron Device Lett.*, vol. 33, no. 4, pp. 480–482, 2012.

[8] T. Grasser, B. Kaczer, W. Goes, T. Aichinger, P. Hehenberger, and M. Nelhiebel, "A Two-Stage Model for Negative Bias Temperature Instability," in *Proc. Intl.Rel.Phys.Symp. (IRPS)*, 2009, pp. 33–44.

[9] Y. Gao, A. Boo, Z. Teo, and D. Ang, "On the Evolution of the Recoverable Component of the SiON, HfSiON and HfO_2 P-MOSFETs under Dynamic NBTI," in *Proc. Intl.Rel.Phys.Symp. (IRPS)*, Apr. 2011, pp. 935–940.

[10] G. Kapila, N. Goyal, V. Maheta, C. Olsen, K. Ahmed, and S. Mahapatra, "A Comprehensive Study of Flicker Noise in Plasma Nitrided SiON p-MOSFETs: Process Dependence of Pre-Existing and NBTI Stress Generated Trap Distribution Profiles," in *Proc. Intl.Electron Devices Meeting (IEDM)*, 2008, pp. 103–106.

[11] B. Kaczer, T. Grasser, J. Martin-Martinez, E. Simoen, M. Aoulaiche, P. Roussel, and G. Groeseneken, "NBTI from the Perspective of Defect States with Widely Distributed Time Scales," in *Proc. Intl.Rel.Phys.Symp. (IRPS)*, 2009, pp. 55–60.

[12] T. Grasser, K. Rott, H. Reisinger, M. Waltl, P. Wagner, F. Schanovsky, W. Goes, G. Pobegen, and B. Kaczer, "Hydrogen-Related Volatile Defects as the Possible Cause for the Recoverable Component of NBTI," in *Proc. Intl.Electron Devices Meeting (IEDM)*, Dec. 2013.

[13] Z. Tung and D. Ang, "Transient to temporarily permanent and permanent hole trapping transformation in the small area sion p-mosfet subjected to negative-bias temperature stress," in *Proc. Intl.Symp. on Physical and Failure Analysis of Integrated Circuits*, 2014, pp. 258–261.

[14] T. Wang, C.-T. Chan, C.-J. Tang, C.-W. Tsai, H. Wang, M.-H. Chi, and D. Tang, "A Novel Transient Characterization Technique to Investigate Trap Properties in HfSiON Gate Dielectric MOSFETs-From Single Electron Emission to PBTI Recovery Transient," *IEEE Trans.Electron Devices*, vol. 53, no. 5, pp. 1073–1079, 2006.

[15] A. Katsetos, "Negative Bias Temperature Instability (NBTI) Recovery with Bake," *Microelectronics Reliability*, vol. 48, no. 10, pp. 1655–1659, 2008.

[16] G. Pobegen and T. Grasser, "On the Distribution of NBTI Time Constants on a Long, Temperature-Accelerated Time Scale," *IEEE Trans.Electron Devices*, vol. 60, no. 7, pp. 2148–2155, 2013.

[17] T. Grasser, B. Kaczer, W. Goes, T. Aichinger, P. Hehenberger, and M. Nelhiebel, "Understanding Negative Bias Temperature Instability in the Context of Hole Trapping," *Microelectronic Engineering*, vol. 86, no. 7-9, pp. 1876–1882, 2009.

[18] Z. Teo, A. Boo, D. Ang, and K. Leong, "On the Cyclic Threshold Voltage Shift of Dynamic Negative-Bias Temperature Instability," in *Proc. Intl.Rel.Phys.Symp. (IRPS)*, 2011, pp. 943–947.

[19] T. Grasser, H. Reisinger, W. Goes, T. Aichinger, P. Hehenberger, P. Wagner, M. Nelhiebel, J. Franco, and B. Kaczer, "Switching Oxide Traps as the Missing Link between Negative Bias Temperature Instability and Random Telegraph Noise," in *Proc. Intl.Electron Devices Meeting (IEDM)*, 2009, pp. 729–732.

[20] T. Grasser, K. Rott, H. Reisinger, M. Waltl, F. Schanovsky, and B. Kaczer, "NBTI in Nanoscale MOSFETs – The Ultimate Modeling Benchmark," *IEEE Trans.Electron Devices*, vol. 61, no. 11, pp. 3586–3593, 2014.

[21] J. Stathis and D. DiMaria, "Identification of an Interface Defect Generated by Hot Electrons in SiO_2," *Appl.Phys.Lett.*, vol. 61, no. 24, pp. 2887–2889, 1992.

[22] J. Campbell, P. Lenahan, C. Cochrane, A. Krishnan, and S. Krishnan, "Atomic-Scale Defects Involved in the Negative-Bias Temperature Instability," *IEEE Trans.Dev.Mat.Rel.*, vol. 7, no. 4, pp. 540–557, 2007.

[23] T. Grasser, W. Goes, Y. Wimmer, F. Schanovsky, G. Rzepa, M. Waltl, K. Rott, H. Reisinger, V. Afanas'ev, A. Stesmans, A.-M. El-Sayed, and A. Shluger, "On the Microscopic Structure of Hole Traps in pMOSFETs," in *Proc. Intl.Electron Devices Meeting (IEDM)*, Dec. 2014.

[24] J. Conley Jr. and P. Lenahan, "Molecular Hydrogen, E′ Center Hole Traps, and Radiation Induced Interface Traps in MOS Devices," *IEEE Trans.Nucl.Sci.*, vol. 40, no. 6, pp. 1335–1340, 1993.

[25] P. Blöchl, "First-Principles Calculations of Defects in Oxygen-Deficient Silica Exposed to Hydrogen," *Physical Review B*, vol. 62, no. 10, pp. 6158–6179, 2000.

[26] J. Stathis and S. Zafar, "The Negative Bias Temperature Instability in MOS Devices: A Review," *Microelectronics Reliability*, vol. 46, no. 2-4, pp. 270–286, 2006.

[27] Y. Mitani, H. Satake, and A. Toriumi, "Influence of Nitrogen on Negative Bias Temperature Instability in Ultrathin SiON," *IEEE Trans.Dev.Mat.Rel.*, vol. 8, no. 1, pp. 6–13, 2008.

[28] V. Huard, "Two Independent Components Modeling for Negative Bias Temperature Instability," in *Proc. Intl.Rel.Phys.Symp. (IRPS)*, May 2010, pp. 33–42.

[29] S. Mahapatra, N. Goel, S. Desai, S. Gupta, B. Jose, S. Mukhopadhyay, K. Joshi, A. Jain, A. Islam, and M. Alam, "A Comparative Study of Different Physics-Based NBTI Models," *IEEE Trans.Electron Devices*, vol. 60, no. 3, pp. 901–916, 2013.

[30] A.-M. El-Sayed, M. Watkins, T. Grasser, V. Afanas'ev, and A. Shluger, "Hydrogen induced rupture of strained Si-O bonds in amorphous silicon dioxide," *Physical Review Letters*, 2015.

[31] D. Griscom, "Diffusion of Radiolytic Molecular Hydrogen as a Mechanism for the Post-Irradiation Buildup of Interface States in SiO_2-on-SiStructures," *J.Appl.Phys.*, vol. 58, no. 7, pp. 2524–2533, 1985.

[32] E. Poindexter, "Chemical Reactions of Hydrogeneous Species in the Si/SiO_2 System," *J. Noncryst. Solids.*, vol. 187, pp. 257–263, 1995.

[33] E. Cartier, J. Stathis, and D. Buchanan, "Passivation and Depassivation of Silicon Dangling Bonds at the $Si(111)/SiO_2$ Interface by Atomic Hydrogen," *Appl.Phys.Lett.*, vol. 63, no. 11, pp. 1510–1512, 1993.

[34] E. Cartier, D. Buchanan, and G. Dunn, "Atomic Hydrogen-Induced Interface Degradation of Reoxidized-Nitrided Silicon Dioxide on Silicon," *Appl.Phys.Lett.*, vol. 64, no. 7, pp. 901–903, 1994.

[35] E. Cartier and J. Stathis, "Atomic Hydrogen-Induced Degradation of the Si/SiO_2 Structure," *Microelectronic Engineering*, vol. 28, no. 1-4, pp. 3–10, 1995.

[36] J. de Nijs, K. Druijf, V. Afanas'ev, E. van der Drift, and P. Balk, "Hydrogen Induced Donor-Type Si/SiO_2 Interface States," *Appl.Phys.Lett.*, vol. 65, no. 19, pp. 2428–2430, 1994.

[37] M. Houssa, V. Afanas'ev, A. Stesmans, M. Aoulaiche, G. Groeseneken, and M. Heyns, "Insights on the Physical Mechanism behind Negative Bias Temperature Instabilities," *Appl.Phys.Lett.*, vol. 90, no. 4, p. 043505, 2007.

[38] M. Wilde and K. Fukutani, "Hydrogen Detection Near Surfaces and Shallow Interfaces with Resonant Nuclear Reaction Analysis," *Surface Science Reports*, vol. 69, no. 4, pp. 196 – 295, 2014.

[39] A. van Duin, S. Dasgupta, F. Lorant, and W. Goddard III, "ReaxFF: A Reactive Force Field for Hydrocarbons," *J.Phys.Chem.A*, vol. 105, no. 41, pp. 9396–9409, 2001.

[40] M. Guidon, J. Hutter, and J. VandeVondele, "Robust Periodic Hartree-Fock Exchange for Large-Scale Simulations Using Gaussian Basis Sets," *J.Chem.Theor.Comp.*, vol. 5, no. 11, pp. 3010–3021, 2009.

[41] Z. Liu, S. Fujieda, H. Ishigaki, M. Wilde, and K. Fukutani, "Current Understanding of the Transport Behavior of Hydrogen Species in MOS Stacks and Their Relation to Reliability Degradation," *ECS Trans.*, vol. 35, no. 4, pp. 55 – 72, 2011.

[42] W. Goes, F. Schanovsky, and T. Grasser, "Advanced Modeling of Oxide Defects," in *Bias Temperature Instability for Devices and Circuits*, T. Grasser, Ed. Springer, New York, 2014, pp. 409–446.

[43] T. Grasser, K. Rott, H. Reisinger, P.-J. Wagner, W. Goes, F. Schanovsky, M. Waltl, M. Toledano-Luque, and B. Kaczer, "Advanced Characterization of Oxide Traps: The Dynamic Time-Dependent Defect Spectroscopy," in *Proc. Intl.Rel.Phys.Symp. (IRPS)*, Apr. 2013, pp. 2D.2.1–2D.2.7.

[44] A. Kerber and E. Cartier, "A Fast Four-Point Sense Methodology for Extraction of Circuit-Relevant Degradation Parameters," *IEEE Electron Device Lett.*, vol. 31, no. 9, pp. 912–914, 2010.

[45] K. Jeppson and C. Svensson, "Negative Bias Stress of MOS Devices at High Electric Fields and Degradation of MNOS Devices," *J.Appl.Phys.*, vol. 48, no. 5, pp. 2004–2014, 1977.

[46] J. McPherson, "Quantum Mechanical Treatment of Si-O Bond Breakage in Silica Under Time Dependent Dielectric Breakdown Testing," in *Proc. Intl.Rel.Phys.Symp. (IRPS)*, 2007, pp. 209–216.

[47] A. Stesmans, "Dissociation Kinetics of Hydrogen-Passivated P_b Defects at the $(111)Si/SiO_2$ Interface," *Physical Review B*, vol. 61, no. 12, pp. 8393–8403, 2000.

[48] L. Tsetseris, X. Zhou, D. Fleetwood, R. Schrimpf, and S. Pantelides, "Hydrogen-Related Instabilities in MOS Devices Under Bias Temperature Stress," *IEEE Trans.Dev.Mat.Rel.*, vol. 7, no. 4, pp. 502–508, 2007.